Time-dependent reactive oxygen species inhibit *Streptococcus mutans* growth on zirconia after a helium cold atmospheric plasma treatment

Yang Yang [a,1], Miao Zheng [b,1], Ya-Nan Jia [c], Jing Li [d], He-Ping Li [e,*], Jian-Guo Tan [f,**]

[a] *Department of Prosthodontics, Peking University School and Hospital of Stomatology, National Clinical Research Center for Oral Diseases, National Engineering Laboratory for Digital and Material Technology of Stomatology, Beijing Key Laboratory of Digital Stomatology, Beijing 100081, PR China*
[b] *Department of Stomatology, Peking University Third Hospital, Beijing 100191, PR China*
[c] *College of Mechanical Engineering, North China University of Science and Technology, Tangshan 063210, PR China*
[d] *Department of Engineering Physics, Tsinghua University, Beijing 100084, PR China*
[e] *Department of Engineering Physics, Tsinghua University, Beijing 100084, PR China*
[f] *Department of Prosthodontics, Peking University School and Hospital of Stomatology, National Clinical Research Center for Oral Diseases, National Engineering Laboratory for Digital and Material Technology of Stomatology, Beijing Key Laboratory of Digital Stomatology, Beijing 100081, PR China*

ARTICLE INFO

ABSTRACT

As an efficient strategy for the modification of material surfaces, cold atmospheric plasma (CAP) has been used in dentistry to improve hard and soft tissue integration of dental implant materials. We previously found the *Streptococcus mutans* growth was inhibited on the surface of zirconia implant abutment after a 60-second helium cold atmospheric plasma treatment. However, the mechanism of bacterial growth inhibition on CAP-treated zirconia has not been fully understood. The duration of bacterial inhibition effectiveness on CAP-treated zirconia has also been insufficiently examined. In this work, we assume that reactive oxygen species (ROS) are the primary cause of bacterial inhibition on CAP-treated zirconia. The ROS staining and an ROS scavenger were utilized to evaluate the bacterial intracellular ROS level, and to determine the role of ROS in bacterial growth inhibition when seeded on CAP-treated zirconia. The time-dependent effectiveness of CAP treatment was determined by changes in surface characteristics and antibacterial efficacy of zirconia with different storage times after CAP treatment. This study confirmed that the presence of reactive oxygen species on the zirconia surface after CAP treatment inhibits the growth of *Streptococcus mutans* on the material surface. Although the antibacterial efficacy of the 60-second CAP-treated zirconia decreased over time, there were fewer bacteria on the treated surface than those on the untreated surface after 14 days.

1. Introduction

The use of dental implants has been established as a routine treatment method to replace missing teeth. Implants with long-term functioning rely not only on solid integration with bones, but also on an intact integration with the surrounding soft tissues. The soft tissue seal around the implant abutment acts as a barrier between the oral environment and the bones underneath, thereby preventing the penetration of oral bacteria and maintaining the normal shape of the gingiva. The constitution of peri-implant soft tissues is similar to that of periodontal tissues. However, there are fewer vascular structures and less

perpendicular fiber bundles in peri-implant soft tissues. The lack of the vascular and fiber bundles leads to a weak connection between peri-implant soft tissues and implant abutments [1]. Therefore, the weakly connected tissues of the implant could be easily influenced and disrupted, thereby eventually leading to bacterial invasion and focal infection. Peri-implant mucositis and peri-implantitis are two plaque-induced biological complications that occur around implants, which further hinder the function and esthetics of implant teeth [2]. The prevalence rate of peri-implantitis differs depending on diagnosis criteria; however, studies have reported that 18.5% of patients and 12.8% of implants suffer from peri-implantitis, while this number is

* Correspondence to: H.-P. Li, Department of Engineering Physics, Tsinghua University, Haidian District, Beijing 100084, PR China.
** Correspondence to: J.-G. Tan, Department of Prosthodontics, Peking University School and Hospital of Stomatology, 22 Zhongguancun South Avenue, Haidian District, Beijing 100081, PR China.
E-mail addresses: liheping@tsinghua.edu.cn (H.-P. Li), kqtanjg@bjmu.edu.cn (J.-G. Tan).
[1] Authors contributed equally to this work.

even higher for peri-implant mucositis [3]. Since the treatment of such diseases is challenging, the early establishment of effective peri-implant soft tissue seal is a good solution to prevent such lesions from emerging.

The human oral cavity consists thousands of bacterial species. Shortly after abutment installation, these contaminating pathogens begin competing in order to cover the abutment surface with soft tissue cells [4]. Streptococcus species, such as *Streptococcus mutans* (*S. mutans*), are some of the earliest colonizers that adhere to the abutment surface, thereby forming a biofilm and providing an adhering matrix for later colonizers [5]. Gristina described this process as the "race for the surface of the implant materials" [6]. In particular, if the bacteria are successful in constituting the majority of the material surface, it will be difficult for soft tissue cells to adhere to the surface, thereby interfering soft tissue barrier formation. However, compared with soft tissue cells, bacteria can quickly attach to the abutment surface with the formation of saliva pellicle [7]. To create a better adhering scenario for soft tissue cells, it is critical to eliminate bacterial growth on the abutment surface. There are several methods to control bacterial contamination on material surface, such as incorporating antibiotics or antimicrobial metallic nanoparticles to the material surface [8,9]. Ideally, the abutment surface should be able to promote soft tissue cell adhesion; meanwhile, it discourages bacterial adhesion, particularly in the early phase of soft tissue wound healing after implant surgery. Numerous studies have focused on this topic, but research on bifunctional surface remains scarce [10].

Zirconium oxide (zirconia) has recently been introduced as a promising implant abutment material owing to its biocompatibility and satisfactory esthetics [11,12]. According to a recent review, zirconia is considered a suitable substitute for the implant abutment material made by titanium [13]. The ivory color of zirconia is favorable in the anterior region. Moreover, studies have demonstrated that it attracts fewer bacteria because of its low surface energy as compared to those of titanium and its alloys [14]. However, as it is a bioinert material, the surface modification of zirconia for a bifunctional goal is still necessary [15]. Recently, the use of cold atmospheric plasma (CAP) has been proposed for promoting soft tissue integration on zirconia abutments [16,17]. Plasma is known as the fourth state of matter, and comprises a partially ionized gas that contains a variety of reactive species. Cold atmospheric plasma is one of the plasma sources generated at atmospheric pressure, which possesses a gas temperature that is similar to the human body temperature [18]. According to our group's previous studies, CAP treatment using helium as the working gas is a promising method to create bifunctional zirconia surfaces. It has been proven useful in promoting human gingival fibroblast cells and inhibiting bacterial growth on zirconia surfaces [19,20]. With the proven effectiveness of surface modification of the material [21], the CAP treatment changes the zirconia surface from hydrophobic to hydrophilic, and the reactive oxygen species (ROS) can be detected on the zirconia surface after CAP treatment.

Reactive oxygen species are known as a source of oxidative stress and are hostile to bacteria [22,23]. Recent studies have demonstrated that an increased intracellular ROS level, which is caused by a direct CAP jet, can either react primarily with the cell envelope or damage intracellular components and subsequently lead to bacterial death [24]. In these types of studies, the bacterial suspension is directly exposed under the CAPs, with the bacterial growth being influenced by the forthright oxidative stress caused by ROS. However, it has not been determined whether the ROS left on the zirconia surface can impose oxidative stress on bacteria after CAP treatment. Therefore, it is important to investigate the mechanisms of bacterial death on the CAP-treated zirconia surface to improve the use of CAP as a promising surface modification method in clinical implant dentistry.

Moreover, soft tissue wound healing around implants requires time [25]. Following implant surgery, the temporal sequence of healing events leads to the integration of the soft tissue integration into the abutment surface. Previously, numerous studies investigating bacterial inhibition on modified abutment surfaces did not evaluate the duration

of the modification effects. Therefore, it is critical to determine the duration time of bacterial inhibition in the process of soft tissue wound healing before clinical usage of the surface modification method. To date, only a few studies have reported the time-dependent effect of CAP-treated zirconia [26,27]. After CAP treatment, the ROS level on the zirconia surface might decrease over time, causing a diminishing effect on bacterial inhibition. Furthermore, the time-dependent change in the surface characteristics of zirconia after CAP treatment, such as hydrophilicity, has not been fully elucidated. Additional studies are needed to further understand the changes in CAP-treated zirconia over time.

In this work, we used ROS staining and ROS scavenging to determine the possible mechanism of bacterial inhibition on the zirconia surface after CAP treatment using helium. The surface characteristic maintaining time and duration of the bacterial inhibition effect of CAP-treated zirconia were also evaluated. *Streptococcus mutans* is one of the most common bacteria in oral cavities, and has been used herein for the antimicrobial tests.

2. Experimental procedures

2.1. Sample preparation

Yttrium-stabilized zirconia disks with 15 mm diameter and 2 mm thickness (Wieland, Pforzheim, Germany) were designed and milled using a computer-aided design and computer-aided manufacturing (CAD-CAM) process. The disks were serially wet-polished using *SiC* abrasive paper until 2000-grit to obtain a unified roughness height of 0.1 μm. All disks underwent an ultrasonic bath in absolute ethanol and deionized water for 20 min. The specimens were naturally dried and stored at room temperature (25 °C) until use.

2.2. Helium CAP jet

An atmospheric-pressure dielectric-barrier-discharge plasma generator was utilized for the zirconia surface modification. Provided by the Plasma Health Scientech Group of Tsinghua University, the detailed schematic diagram of the device has been provided in previous studies [20,28]. In this study, the CAP jet was generated by using high-purity helium as the plasma working gas at a flow rate of 13.5 slpm. The discharge voltage and driving frequency of the power supply were set to 2.85 kV and 17.0 kHz, respectively. For CAP surface treatment, the zirconia disk was placed on the sample stage co-axially with the geometrical axis of the plasma jet, while the distance between the zirconia surface and the nozzle exit of the plasma generator was maintained at 1.0 cm. The disk was fixed and treated by the CAP jet for 60 s, and then subjected to the tests.

2.3. Bacterial culture

2.3.1. Bacterial suspension

Gram-positive bacteria *Streptococcus mutans* (UA159) was provided by the Institute of Microorganisms, Chinese Academy of Science. The bacteria were maintained on a brain-heart infusion (BHI, BD-Difco, USA) agar plate and incubated at 37 °C in a humidified atmosphere of 5% CO_2 and 95% air. A monoclonal colony was transferred to 10 ml of the BHI broth culture medium and cultured to the exponential phase for use. Prior to the experiments, bacterial cells were centrifuged at 3000 $\times g$ for 15 min. The bacterial pellet was washed twice with 0.1 M PBS buffer (Solarbio, China) and adjusted to a final concentration of 1×10^8 CFU/ml. Before seeding, the suspension was shaken for 30 s (Vortex 2, IKA, Germany) to obtain single cells or pairs, and then seeded on the sterilized samples in 24-well plates for further experiments.

2.3.2. ROS scavenger pre-treatment

To determine the ROS-induced bacterial inhibition mechanism on the CAP-treated zirconia surface, a ROS scavenger was used. *N*-acetyl-L-

cysteine (NAC, Sigma-Aldrich, USA) is a ROS scavenger that is considered to inhibit ROS-induced cell apoptosis [29]. The bacteria are protected by excessive oxidative stress when NAC is present. To obtain the NAC-treated bacterial suspension, 10 mM NAC was added to the bacterial suspension and cultivated for 2 h before seeding to the zirconia surface.

2.4. Study design

This study consists of two parts. In the first part, possible mechanisms of bacterial inhibition of CAP-treated zirconia were explored. In the second part, the changes in surface characteristic of zirconia over time and its bacterial inhibition efficacy were tested. Detailed flowcharts of the study are shown in Schemes 1 and 2. Zirconia disks were randomly allocated to different groups, and three parallel samples were tested in each group. All experiments were repeated three times.

Details of the experimental groups are following:

Negative control group: Zirconia disks with no treatment.
Positive control group: 0.1 mM H_2O_2 added to the zirconia surface. H_2O_2, which is known as an ROS inducer, increases bacterial intracellular ROS levels.
CAP group: Zirconia disks with 60 s CAP treatment.
CAP+NAC group: Zirconia disks with 60 s CAP treatment, and the NAC-treated bacteria were seeded.
H_2O_2 + NAC group: 0.1 mM of H_2O_2 was added to the zirconia surface, and the NAC-treated bacteria were seeded.
CAP baseline group: Zirconia disks with 60 s CAP treatment were immediately subjected to the tests.
CAP n-day group: Zirconia disks with 60 s CAP treatment were subjected to tests after storage in the dark at 37 °C for n days.

2.5. Zirconia morphological changes after CAP treatment

The morphological changes before and after CAP treatment were evaluated by a field emission scanning electron microscope (FE-SEM; S-8010, Hitachi, Japan). Samples from the negative control group and CAP group were naturally dried, sputter-coated with gold, and subjected to FE-SEM observations.

2.6. Intracellular ROS staining assay

The intracellular ROS level of bacteria was determined using the fluorescent probe, 2′,7′-dichlorodihydrofluorescein diacetate (DCFH-DA, Beyotime, China), which could be deacetylated and oxidized to fluorescent products after passing through the membrane of the live bacteria. The bacteria were seeded onto the zirconia surface and cultivated for 3 h. After discarding the growth medium, the disks were washed three times with PBS, and 10 μM DCFH-DA was added to the zirconia surface. Following cultivation at 37 °C in the dark for 15 min, the excess dye was removed by PBS. The stained bacteria were observed using a confocal laser scanning microscope (CLSM; LSM710, Zeiss, Germany) at 40-fold magnification. Cells with high levels of intracellular ROS were observed to be green-fluorescent.

### 2.7. Bacteria viability and morphology observation

To evaluate bacterial viability, the LIVE/DEAD BacLight bacterial viability staining kit (L-7012, Invitrogen, USA) was used. The dye was premixed using SYTO 9, propidium iodide, and PBS at a volume ratio of 1.5:1.5:1000. The bacteria were seeded onto the zirconia surface and cultivated for 24 h. After discarding the culture medium, bacterial cells were washed three times with PBS, and then 300 μl of mixed staining dye was added to the sample. After 15 min of incubation at 37 °C in the dark, the stained bacteria were observed using CLSM at 40-fold magnification. The live cells were observed to be green-fluorescent and dead cells were observed red-fluorescent.

The FE-SEM was utilized again to observe the bacterial morphology. After 24-hour cultivation, the culture medium was discarded; the bacteria were washed three times using PBS and then fixed with 2.5% glutaraldehyde (Solarbio, China) overnight at 4 °C. Specimens were dehydrated through a graded series of ethanol (30, 60, 90, 95, 100%, v/v), naturally dried, sputter-coated with gold, and subjected to FE-SEM observations.

2.8. Quantitative bacterial adhesion assay and biofilm formation assay

To quantitatively analyze the bacterial adhesion on the zirconia surface, the MTT (3-(4,5-dimethylthiazol-2-yl)-2,5-diphenyltetrazolium bromide) colorimetric assay was utilized. The MTT assay is based on the cleavage of MTT into a blue formazan by living cell enzymes, and the formation of formazan is positively correlated with adhered living cells. MTT solution was prepared by dissolving 5 mg/ml of MTT (Biosynth, USA) in PBS. After seeding bacteria to the zirconia surface and cultivating, the culture medium was discarded, and the zirconia disks were washed three times with PBS to remove non-attached bacteria cells. Five microliters of MTT solution and 500 μl of broth were added to the zirconia and incubated in the dark for 3 h at 37 °C. The formazan formed was dissolved by adding 500 μl DMSO (ThermoFisher Scientific, USA), and the optical density of the final solution was determined at 570 nm using a microplate reader (ELX808, BioTek, USA).

To investigate the total biofilm formation, a crystal violet (CV) assay was used. After seeding bacteria to the zirconia surface and cultivating, the culture medium was discarded. The zirconia disks were washed three times with PBS, air-dried, and fixed with 2.5% glutaraldehyde for 20 min. The fixed bacterial biofilm was stained using 1% crystal violet
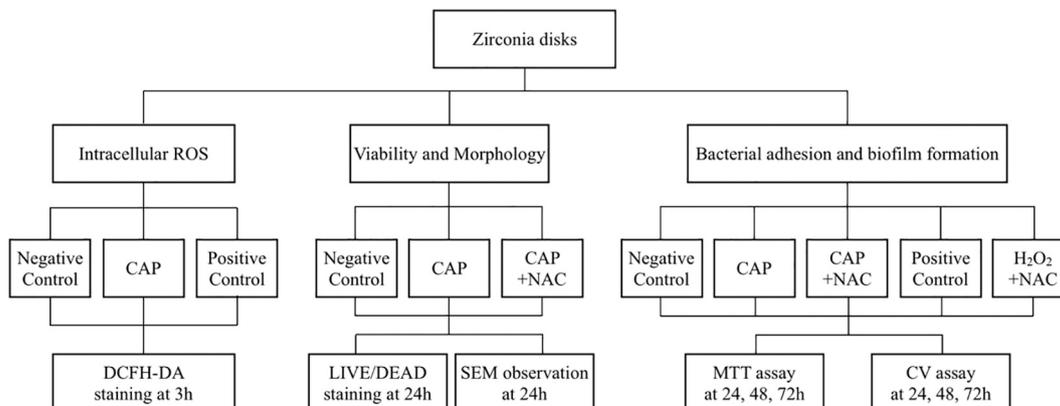
Scheme 1. Flowchart of mechanism evaluation of bacterial inhibition on CAP-treated zirconia.
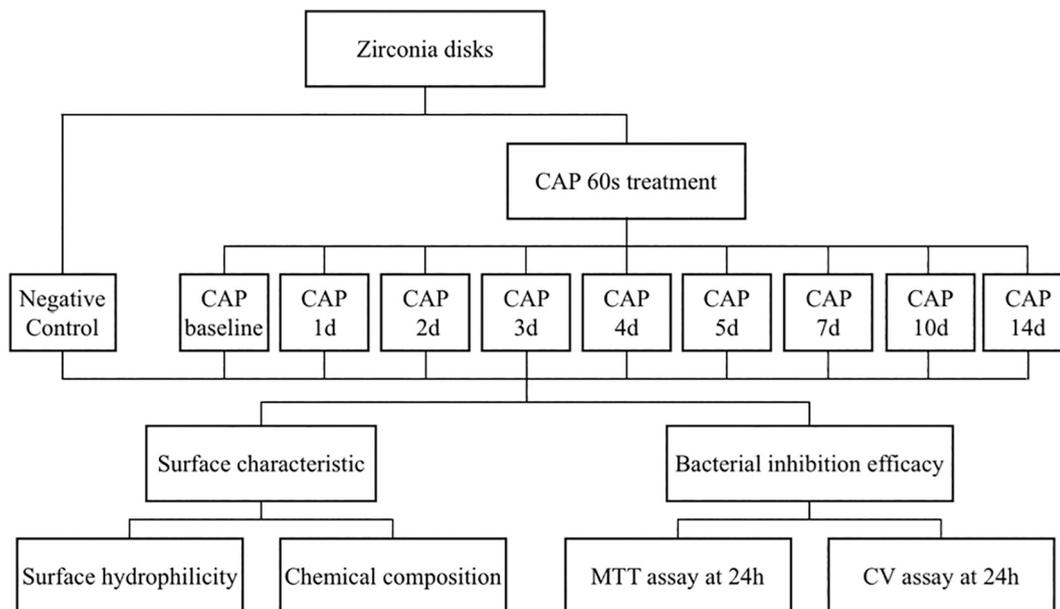
Scheme 2. Flowchart of the evaluation of time-dependent change of CAP-treated zirconia.

solution (Sigma-Aldrich, MO, USA) followed by a 10-min incubation at room temperature. After washing the unbound dye with gentle running deionized water, the bound CV was extracted using absolute ethanol. The amount of biofilm was measured at 570 nm using a microplate reader.

2.9. Time-dependent surface characteristic change analysis

To examine the changes in the surface characteristics of CAP-treated over time, the surface hydrophilicity and chemical composition were analyzed. The surface hydrophilicity was determined by measuring the contact angle of 1 μl of deionized water droplets on the zirconia surface with different storage times, using a contact-angle-measuring device (OCA15EC, Dataphysics, Germany). Measurements were taken at five different locations on each of the three samples per group.

The chemical composition of the surfaces was analyzed by X-ray photoelectron spectroscopy (XPS; ESCALAB 250, ThermoFisher Scientific, USA). The binding energies were referenced to the C 1s peak at 284.6 eV.

2.10. Statistical analysis

All data are expressed as mean ± standard deviations. Statistical analysis was performed by one-way ANOVA using SPSS software (Version 25, IBM, USA). $p < 0.05$ was considered statistically significant.

3. Results and discussion

3.1. Zirconia surface before and after CAP treatment

The FE-SEM results show no significant changes before and after CAP treatment. As shown in Fig. 1, zirconia specimens from both the negative control group and the CAP group possess similar morphologies with typical ground marks, which resulted from the grinding process. This result confirms that the 60-second helium CAP treatment in this study did not change the zirconia morphology.

3.2. Increased bacterial intracellular ROS level by seeding on CAP-treated zirconia

In our previous study, a rich level of ROS remained on the zirconia surface after the CAP treatment, as detected by the surface chemical analysis [20]. To determine whether these reactive species interact with bacterial cells, the ROS staining assay was performed using DCFH-DA. As shown in Fig. 2, CAP-treated zirconia significantly increased the bacterial intracellular ROS level. The results were similar to the effect of hydrogen peroxide, which was used as a positive control. These combined results show that CAP-treated zirconia can increase the
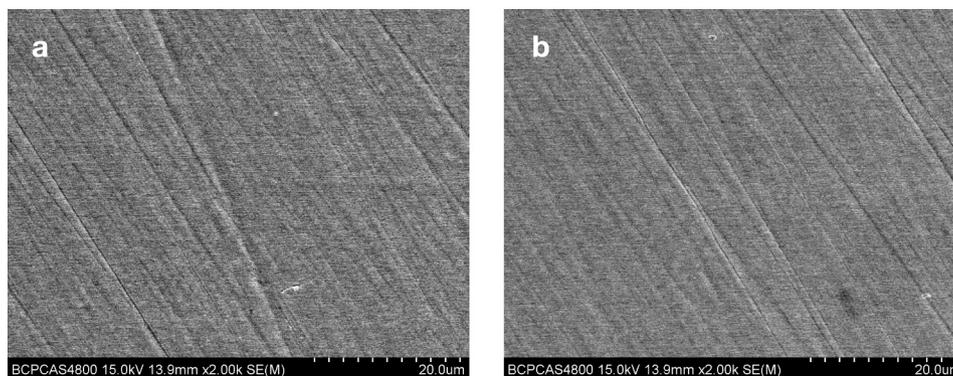
Fig. 1. SEM images of zirconia surfaces from negative control (a) and CAP (b) group. (2k magnification).
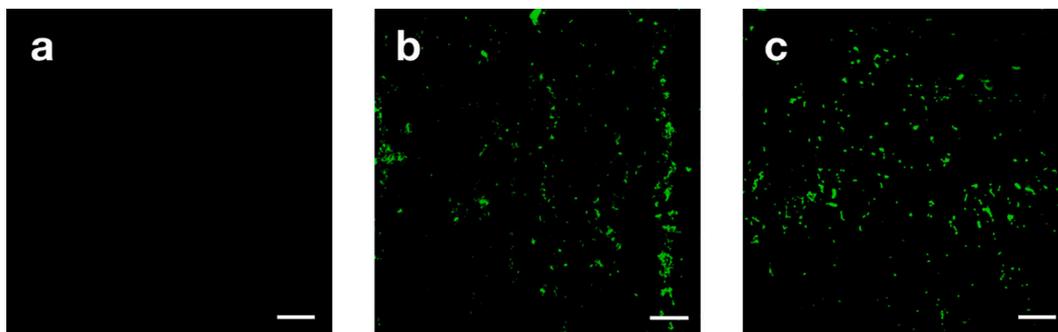
Fig. 2. DCFH-DA staining of the negative control (a), CAP (b), and positive control (c). Scale bar is 20 μm.

intracellular ROS level in bacteria.

Cold atmospheric plasma is known to directly inactivate a variety of bacteria, while antimicrobial resistance caused by CAP is reported to be less than that caused by antibiotics [30], thereby suggesting that CAP is a useful way to control infection. When bacteria are directly exposed to CAP, the combined effects of ultraviolet radiation, electric fields, and reactive species work synergistically to inactivate bacteria [31]. However, this is different from the CAP-treated material, since the bacteria interact with the modified material surface by CAP, rather than CAP itself. Through ROS staining assay, it can be inferred that ROS left on zirconia after CAP treatment interacts with *S. mutans* after 3-hour cultivation, and these ROS might contribute to the death of the bacteria.

3.3. Decreased bacterial inhibition effect of CAP-treated zirconia with the presence of ROS scavenger

Previous studies have demonstrated that ROS causes bacterial cell death [24]. As the intracellular ROS level was elevated in *S. mutans*, we aimed to determine whether intracellular ROS is the primary cause of bacterial death on CAP-treated zirconia. Therefore, the ROS scavenger (NAC) was used. NAC is a synthetic precursor of intracellular cysteine and glutathione, and its anti-ROS activity results from its free radical scavenging property either directly *via* the redox potential of thiols, or indirectly by increasing glutathione levels in the cells [29].

The viability of bacteria with or without pretreatment with NAC was determined using the LIVE/DEAD assay, with the viable bacteria cells being stained green and the inviable bacterial cells being stained red. As shown in Fig. 3, CAP treatment induced significant bacterial cell death. However, this was reverted by the NAC treatment, suggesting that increased intracellular ROS levels are the cause of cell death. The same trend was observed in the positive control and H_2O_2 + NAC groups, which provided further evidence for the role of ROS in surface antibacterial properties. Remarkably, an enhanced biofilm formation with a sophisticated spatial structure was observed in the CAP+NAC treatment group.

FE-SEM was also utilized to investigate bacterial morphology (Fig. 4). Compared with the negative control group, a total decrease in bacterial load was observed on the CAP surface and the surface of the

positive control group. Furthermore, the bacteria on the CAP and on the surfaces of the positive control groups were more scattered, which indicated that the reproduction ability of bacteria was hindered. After adding the bacteria pretreated with NAC to the CAP group, the surface antimicrobial effect was reversed; consequently, the bacteria presented a dense and connected structure, which was in accordance with the LIVE/DEAD staining results. The results of the H_2O_2 + NAC group further confirmed the rescuing effect of NAC on bacterial growth. Moreover, it is worth noting that the change in bacterial morphology change among the five groups was not distinctive. This can be attributed to the indirect contact with the CAP jet for bacterial cells. Furthermore, as dead or non-adhering bacterial cells were washed out prior to FE-SEM testing, only living bacteria with intact morphology were observed during the test.

To further evaluate the bacterial adhesion, growth, and biofilm formation under the effect of the ROS scavenger, quantitative assays were performed. The adhesion and growth of *S. mutans* was investigated using MTT assays. As shown in Fig. 5, the bacterial adhesion and growth on the CAP-treated zirconia surface were significantly inhibited after 24-hour cultivation, and this effect persisted after 72 h. However, when NAC was added, the bacterial adhesion and growth on the CAP-treated surface returned to normal. The tested OD value of the CAP+NAC group was even higher than that of the negative control group after 24-hour cultivation. The positive control/H_2O_2 + NAC group showed a similar trend as that of the CAP/CAP+NAC group.

Biofilm formation in different groups was evaluated using crystal violet assays. A similar trend was observed as bacterial adhesion and growth tests by MTT assays. As shown in Fig. 6, compared with the negative control group, fewer biofilm masses were formed by *S. mutans* when seeding to the CAP-treated zirconia; however, more masses were formed when ROS scavenger was present. After cultivating for 24 or 48 h, bacteria in the CAP+NAC group produced more biofilm masses than those achieved with the negative control group.

In the presence of the ROS scavenger, bacterial adhesion, growth, and biofilm formation were no longer inhibited by CAP treatment, indicating that increased intracellular ROS levels are the cause of bacterial death on CAP-treated zirconia. The MTT assay and crystal violet assay results confirmed that the bacteria treated with NAC on the CAP-
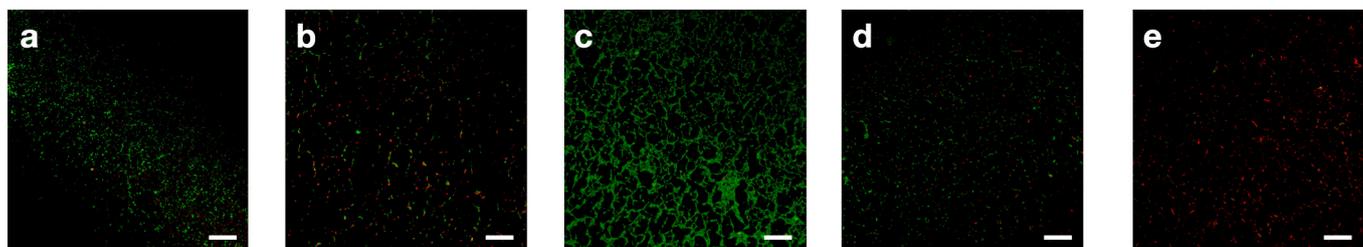

Fig. 3. LIVE/DEAD staining results after 24-hour cultivation for the negative control (a), CAP (b), CAP+NAC (c), H_2O_2 + NAC (d), and positive control (e) group. Scale bar is 20 μm.
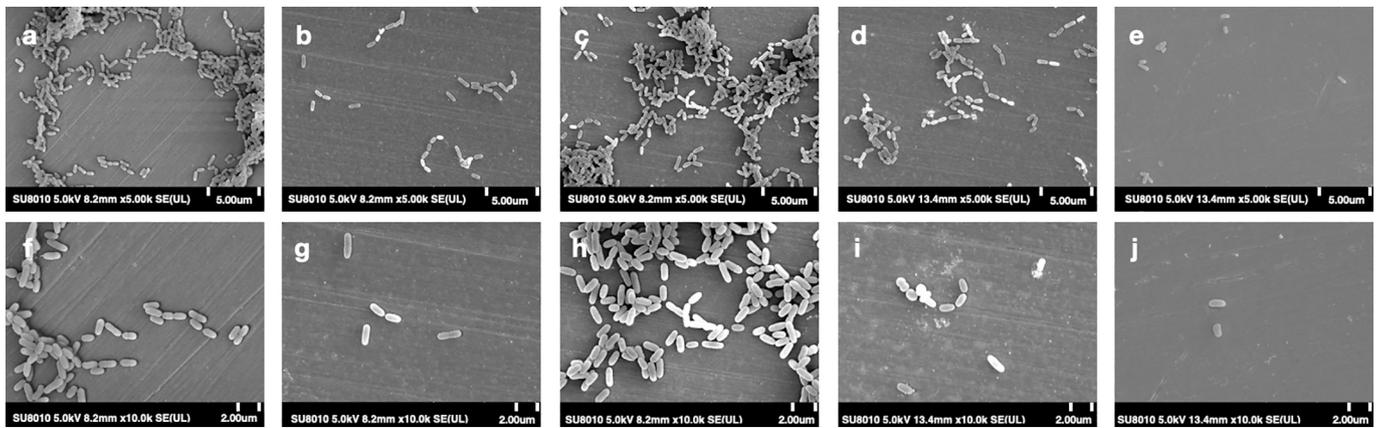
Fig. 4. SEM images of negative control (a,f), CAP (b,g), CAP+NAC (c,h), H_2O_2 + NAC (d,i), and positive control (e,j) group. (One for 5k magnification and one for 10k magnification).
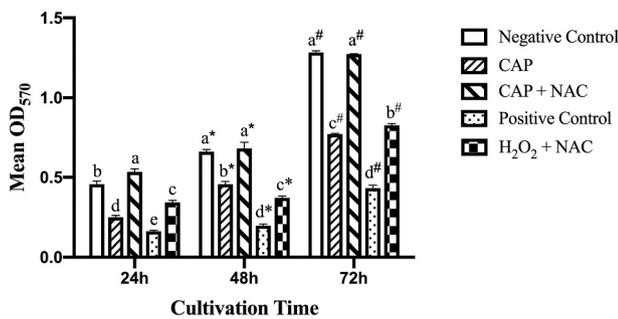

Fig. 5. MTT assay results of *S. mutans* with or without ROS scavenger. (Values indicated by the same letters are not significantly different) ($p > 0.05$).
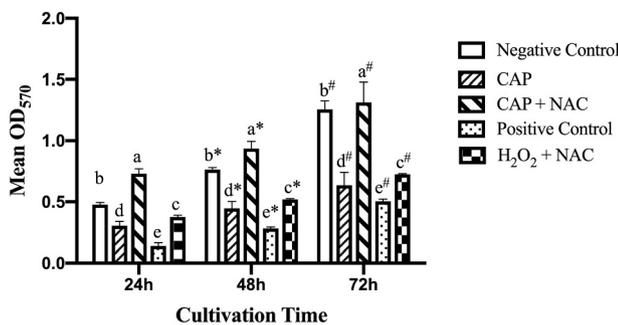

Fig. 6. Crystal violet assay results of *S. mutans* with or without ROS scavenger. (Values indicated by the same letters are not significantly different) ($p > 0.05$).

treated surface grew better than the negative group, with an increased production of biofilm masses just after 24-hour cultivation. This phenomenon can be attributed to the hydrophilicity of the zirconia surface; after CAP treatment, the zirconia disks become more hydrophilic, with an increased surface free energy. Such surfaces favor the adhesion of bacteria with high membrane surface energies. *S. mutans* possess high membrane surface energy, according to previous study [32]. Therefore, after CAP treatment, its adhesion to a more hydrophilic zirconia surface was facilitated, while bacterial death was simultaneously avoided in the presence of the ROS scavenger. This is also the possible cause of a fewer number of bacterial deaths, although a higher bacterial load can be observed through LIVE/DEAD staining after 24-hour cultivation; further, a dense biofilm was formed on the CAP+NAC group, as indicated by the bacterial morphological observation.

The positive control group and H_2O_2 + NAC group results further

confirmed the hostility of ROS toward bacteria and the role of NAC role in protecting the bacteria from oxidative stress. Hydrogen peroxide, a ROS inducer, is frequently added to the culture media to exert ambient oxidative stress on bacteria [33]. In this study, hydrogen peroxide was added to the culture media to mimic the situation of reactive species lingering on the zirconia surface. In the ROS staining assay, green fluorescence was observed in the positive control group, indicating that hydrogen peroxide can raise intracellular ROS levels in *S. mutans*. The bacterial growth inhibition observed in the MTT assay, the decreased biofilm formation in the crystal violet assay, and their reversed results after seeding NAC-treated bacteria proved the occurrence of bacterial death and the rescue process between the ROS and ROS scavengers. Moreover, the results of the H_2O_2 + NAC and CAP+NAC groups also support the hypothesis that CAP treatment leads to a hydrophilic surface that enhances bacterial adhesion and biofilm formation. As adding H_2O_2 does not improve the zirconia surface hydrophilicity, adding NAC-treated bacteria to the H_2O_2 surface will not lead to the flourishing of bacterial growth and biofilm production.

In this study, the reactive oxygen species is one of the causes of bacterial growth inhibition on CAP-treated zirconia. As free radical species, ROS play a vital role in numerous cellular physical processes [34,35]. Since there are different intracellular ROS levels in different cells [36], the key to achieving antimicrobial effect without interfering with normal cell growth is to modify the material surface with a proper amount of ROS. We previously reported that 60-second CAP treatment enhances human gingival fibroblast growth without any adverse effects [19]. With this study further confirming its hostile effect on *S. mutans*, the 60-second CAP treatment method has good potential for future clinical use. The ROS produced using the 60-second CAP treatment exceeds the threshold for *S. mutans*, but is within the limits of human gingival fibroblasts.

3.4. Surface characteristic and bacterial inhibition efficacy change over time

The goal of the surface modification method of zirconia is to create a bifunctional surface to promote soft tissue integration around the implant abutment, preventing peri-implant lesions from occurring. After implant placement and abutment installation, soft tissue follows a certain sequence to heal and reestablish structures under a specific period of time. It is believed that soft tissues approximately require two weeks to form a primary seal by gingival epithelial [37]. Until the primary seal is formed, the bacteria control around the implant is realized by the patient using mouth rinses and taking antibiotics regularly. However, while systematic administration of antibiotics does not aim for a precise target and might introduce antimicrobial resistance, local

usage of antibacterial agents might have certain side effects. The CAP-treated zirconia abutment surface can solve these issues without causing further complications. The only question is, whether the surface modification of zirconia by CAP will last for a sufficient period and facilitate the formation of the primary seal around the implant. Therefore, the duration of zirconia surface characteristics was evaluated along with the retained bacterial inhibition efficacy after the CAP treatment.

The surface hydrophilicity and surface chemical composition were tested after different storage lengths to determine the changes in the surface characteristic of the CAP-treated zirconia over time. The surface hydrophilicity results of the CAP-treated zirconia are shown in Fig. 7. Immediately after CAP treatment, the water contact angle of the zirconia surface decreased significantly from 80.5° ±1.5° to 43.5° ±1.4°, thereby suggesting a more hydrophilic surface was created using the CAP treatment. With time, the water contact angle of zirconia slowly increased. On the 7th day, the surface water contact angle was 60.9° ±1.8°, while this number continued to increase to 68.8° ±3.5° after 14 d storage. The CAP-treated zirconia surface remained moderately hydrophilic after two weeks.

The XPS analysis revealed the changes in the chemical composition of the CAP-treated zirconia surface. The atomic percentage of the surface is shown in Table 1. After the plasma treatment, the percentage of oxygen increased from 36.02% to 53.12%, with a carbon/oxygen ratio decreasing from 1.34 to 0.53. As the storage time increased, the surface oxygen percentage showed a decreasing tendency, while an increase in the carbon/oxygen ratio. For the 14-day storage group, the surface oxygen percentage decreased to 43.78%, which was higher than that of the negative control group. For all the CAP-treated groups, a peak at 532.5 eV can be detected in the high-resolution oxygen results (Fig. 8), which represent the oxygen in the hydroxide state.

To evaluate the time-dependent bacterial inhibition efficacy of CAP-treated zirconia, MTT assays were performed to evaluate bacterial adhesion and growth, while crystal violet assays were performed to evaluate the total amount of biofilm generated. Figs. 9 and 10 show that the ability to inhibit bacterial adhesion, growth, and biofilm formation of CAP-treated zirconia was gradually lost.

The fading of the antibacterial effect is possible because of the extinction of reactive oxygen species on the zirconia surface, as shown by the surface chemical composition tests. The XPS tests show that the oxygen percentage on the CAP-treated zirconia surface slowly decreases, while the carbon percentage increases simultaneously. This also explains why the water contact angle of the zirconia surface is increased daily, as Rupp et al. reported that hydrophobic hydrocarbon chemicals in the environment might contaminate the zirconia surface and increase surface hydrophobicity with time [38]. Nevertheless, until the 14th day, the CAP-treated zirconia surface remained moderately hydrophilic, with ROS still detectable via XPS tests. The MTT assay and crystal violet assay results show that bacterial adhesion and biofilm formation on the 14-day zirconia surfaces are statically less significant compared to those
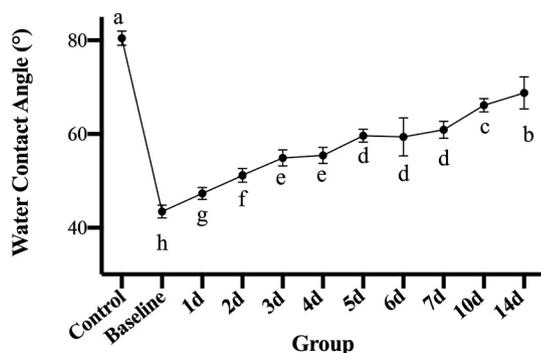
Table 1
Atomic percentage of C1s and O1s on zirconia surfaces.

	C1s (%)	O1s (%)	C/O ratio
Negative control	48.19	36.02	1.34
CAP baseline	27.77	53.12	0.53
CAP 1d	37.68	46.18	0.82
CAP 3d	38.09	46.13	0.83
CAP 5d	40.52	44.05	0.92
CAP 7d	40.88	43.06	0.95
CAP 10d	41.55	43.82	0.95
CAP 14d	42.50	43.78	0.97

on the negative control group. These results show that CAP-treated zirconia retains certain bacterial inhibition efficacy after two weeks of storage as compared with untreated groups. These results imply that the ROS still play a certain role in bacterial growth inhibition on CAP-treated zirconia after 14 d. Notably, the highest bacterial inhibition efficacy of zirconia was observed in the baseline group, suggesting that immediate usage after CAP treatment would be the optimal circumstance for future clinical application. Since the initial bacterial colonization occurs approximately around 2 h after implant abutment installation [4], the strong antimicrobial effect in the first several hours, and even in the first several days, can effectively eliminate the bacterial growth on the abutment surface.

Several studies have also evaluated the timeliness of CAP treatment on zirconia or other biocompatible materials, such as titanium. However, no consensus has been reached. Vilas et al. reported a decrease in the water contact angle of zirconia within 48 h after the argon CAP treatment [27], while Park et al. also reported that the antimicrobial efficacy of zirconia against *S. mutans* lasts for two days after the argon CAP treatment [26]. For CAP-treated titanium, Monetta et al. reported that the antimicrobial activity of titanium is be detected to be at the same level as those of the immediately treated samples after the oxygen CAP treatment for 16 days [39]. Choi et al. reported that compressed air CAP-treated titanium samples are sufficient to promote the alkaline phosphatase activity of MC3T3-E1 pre-osteoblast cells after seven days of incubation, while the surface remained more hydrophilic compared to untreated samples even after 28 d [40]. The inconsistency among the reported studies can be attributed to different CAP treatment processes. As the CAP configuration, working gas, treatment time, and doses vary among studies, it is difficult to compare different studies and reach a definitive conclusion. Under our experimental settings, the helium CAP modification on zirconia has been proven useful in bacterial inhibition for at least two weeks, which fulfills the minimum time required to form a primary soft tissue barrier. Although the CAP treatment does not offer long-lasting antibacterial effects like other antimicrobial agents [8,9], it is still an effective surface modification method, particularly during the early stage of peri-implant wound healing. Moreover, the 60-second chairside CAP treatment can be conveniently completed by dentists or dental technicians, and is therefore considered as easy and efficient tool in future clinical applications.

This study has several limitations. First, as an *in vitro* study, the culture situation set in this study did not completely comply with the real circumstances in the oral cavity. Moreover, as only one antioxidant, NAC, was employed to demonstrate the involvement of ROS in the bacterial inhibition mechanism; the authors have been very careful in interpreting the data. This study does not fully confirm that ROS is the definitive cause of bacterial inhibition of CAP-treated zirconia; however, it does report the involvement of ROS in the death of *S. mutans* death on CAP-treated zirconia. To further investigate the concrete mechanisms, more research is needed to define and identify the bacterial death signaling pathways induced by ROS. Moreover, more cytocompatibility tests should be performed to facilitate the use of CAP-treated zirconia as a human implantation material [41,42]. Therefore, co-culture studies using human gingival fibroblasts and human oral bacteria are needed in future research [43].
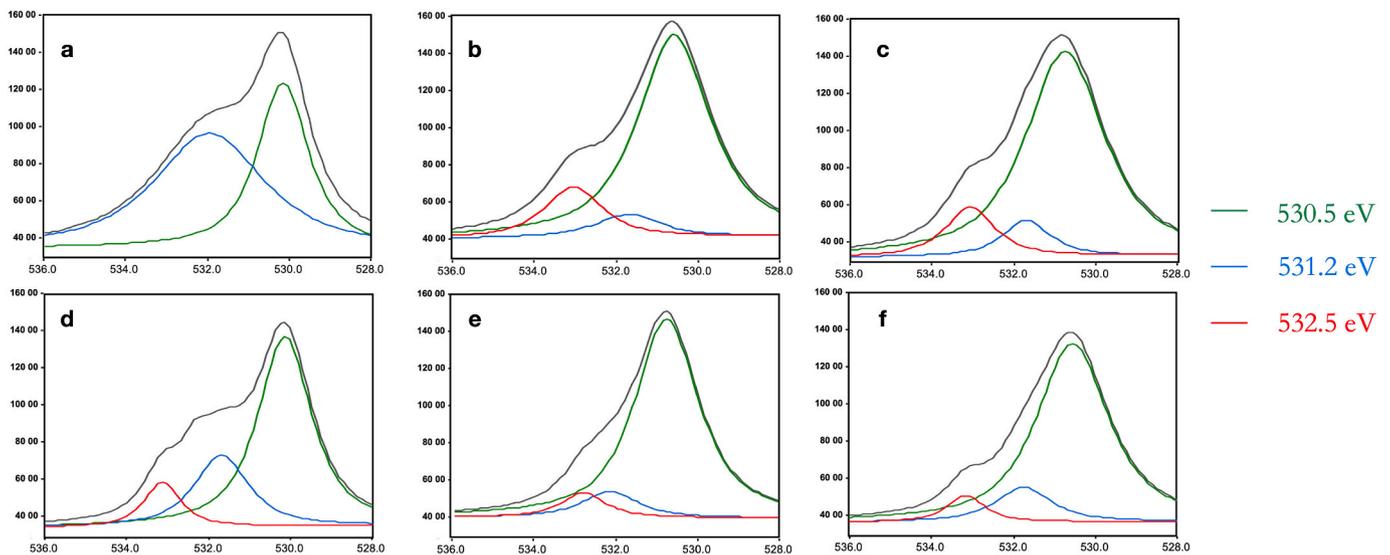

Fig. 7. Water contact angles at the zirconia surface over time. (Values indicated by the same lowercase letters are not significantly different) ($p > 0.05$).

Fig. 8. XPS O1s high-resolution image of the negative control (a), CAP baseline (b), CAP 1d (c), CAP 5d (d), CAP 10d (e), and CAP 14d (f). X axis: Binding energy, Y axis: Counts.
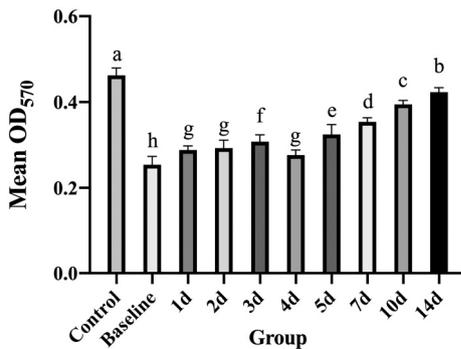

Fig. 9. MTT assay results of the time-dependent CAP treatment effect. (Values indicated by the same lowercase letters are not significantly different) ($p > 0.05$).

Fig. 10. Crystal violet assay results of the time-dependent CAP treatment effect. (Values indicated by the same lowercase letters are not significantly different) ($p > 0.05$).

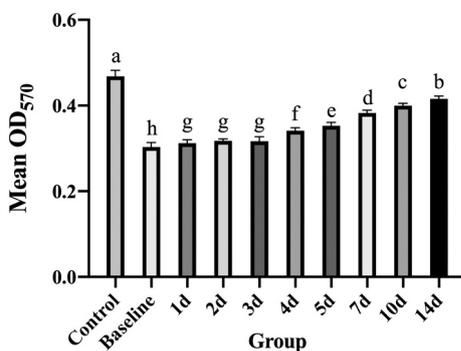## 4. Conclusions

In summary, this study determined that the reactive oxygen species offer a potential mechanism for inhibiting the growth of *S. mutans* growth on the zirconia surface treated by helium cold atmospheric plasma. Moreover, the study also found that after a 60-second helium cold atmospheric plasma treatment, the bacterial inhibition efficacy of

zirconia decreases over time. However, after two weeks of incubation, the zirconia disks still possess a certain bacterial inhibition ability as compared to the untreated disks.

CRediT authorship contribution statement

Yang Yang and Miao Zheng: Investigation, Data curation, Writing – original draft.

Jing Li and Ya-Nan Jia: Validation, Visualization, Writing – review and editing.

Jian-Guo Tan and He-Ping Li: Conceptualization, Methodology, Funding, Writing – review and editing.

Declaration of competing interest

The authors declare that they have no known competing financial interests or personal relationships that could have appeared to influence the work reported in this paper.

Acknowledgements

References

[1] S. Ivanovski, R. Lee, Comparison of peri-implant and periodontal marginal soft tissues in health and disease, Periodontol 2000 (76) (2018) 116–130, https://doi.org/10.1111/prd.12150.

[2] T. Berglundh, G. Armitage, M.G. Araujo, G. Avila-Ortiz, J. Blanco, P.M. Camargo, Peri-implant diseases and conditions: consensus report of workgroup 4 of the 2017 world workshop on the classification of periodontal and peri-implant diseases and conditions, J. Clin. Periodontol. 89 (Suppl. 1) (2018) S313–S318, https://doi.org/10.1002/JPER.17-0739.

[3] M. Rakic, P. Galindo-Moreno, A. Monje, S. Radovanovic, H.-L. Wang, D. Cochran, et al., How frequent does peri-implantitis occur? A systematic review and meta-analysis, Clin. Oral Investig. 22 (2017) 1805–1816, https://doi.org/10.1007/s00784-017-2276-y.

[4] R.P. Jordan, L. Marsh, W.N. Ayre, Q. Jones, M. Parkes, B. Austin, et al., An assessment of early colonisation of implant-abutment metal surfaces by single species and co-cultured bacterial periodontal pathogens, J. Dent. 53 (2016) 64–72, https://doi.org/10.1016/j.jdent.2016.07.013.

[5] M. Quirynen, C.M. Bollen, The influence of surface roughness and surface-free energy on supra- and subgingival plaque formation in man, A review of the literature, J Clin Periodontol. 22 (1995) 1–14, https://doi.org/10.1111/j.1600-051x.1995.tb01765.x.

[6] A. Gristina, Biomaterial-centered infection: microbial adhesion versus tissue integration, Science. 237 (1987) 1588–1595, https://doi.org/10.1111/10.1126/science.3629258.

[7] M.M. Fürst, G.E. Salvi, N.P. Lang, G.R. Persson, Bacterial colonization immediately after installation on oral titanium implants, Clin. Oral Implants Res. 18 (2007) 501–508, https://doi.org/10.1111/j.1600-0501.2007.01381.x.

[8] M.Q. Khan, D. Kharaghani, Sanaullah, A Shahzad, NP Duy, Y Hasegawa, et al, Fabrication of antibacterial nanofibers composites by functionalizing the surface of cellulose acetate nanofibers, ChemistrySelect. 5 (2020) 1315–1321, https://doi.org/10.1002/slct.201901106.

[9] M. Hashmi, S. Ullah, I.S. Kim, Copper oxide (CuO) loaded polyacrylonitrile (PAN) nanofiber membranes for antimicrobial breath mask applications, Curr Res Biotechnol. 1 (2019) 1–10, https://doi.org/10.1016/j.crbiot.2019.07.001.

[10] M-N Abdallah, Z Badran, O Ciobanu, N Hamdan, F Tamimi, Strategies for optimizing the soft tissue seal around osseointegrated implants, Adv Healthc Mater. 6 (2017). doi:https://doi.org/10.1002/adhm.201700549.

[11] M.B. Blatz, M. Bergler, S. Holst, M.S. Block, Zirconia abutments for single-tooth implants—rationale and clinical guidelines, J Oral and Maxillofac Surg. 67 (2009) 74–81, https://doi.org/10.1016/j.joms.2009.07.011.

[12] J.L. Pozzobon, G.K.R. Pereira, V.F. Wandscher, L.S. Dorneles, L.F. Valandro, Mechanical behavior of yttria-stabilized tetragonal zirconia polycrystalline ceramic after different zirconia surface treatments, Mater. Sci. Eng. C Mater. Biol. Appl. 77 (2017) 828–835, https://doi.org/10.1016/j.msec.2017.03.299.

[13] K. Sivaraman, A. Chopra, A.I. Narayan, D. Balakrishnan, Is zirconia a viable alternative to titanium for oral implant? A critical review, J Prosthodont Res. 62 (2018) 121–133, https://doi.org/10.1016/j.jpor.2017.07.003.

[14] A.S.D. Al-Radha, D. Dymock, C. Younes, D. O'Sullivan, Surface properties of titanium and zirconia dental implant materials and their effect on bacterial adhesion, J. Dent. 40 (2012) 146–153, https://doi.org/10.1016/j.jdent.2011.12.006.

[15] F.H. Schünemann, M.E. Galárraga-Vinueza, R. Magini, M. Fredel, F. Silva, J.C. M. Souza, et al., Zirconia surface modifications for implant dentistry, Mater. Sci. Eng. C Mater. Biol. Appl. 98 (2019) 1294–1305, https://doi.org/10.1016/j.msec.2019.01.062.

[16] H.-P. Li, X.-F. Zhang, X.-M. Zhu, M. Zheng, S.-F. Liu, X. Qi, et al., Translational plasma stomatology: applications of cold atmospheric plasmas in dentistry and their extension, High Volt. 2 (2017) 188–199, https://doi.org/10.1049/hve.2017.0066.

[17] W.L. Hui, V. Perrotti, F. Iaculli, A. Piattelli, A. Quaranta, The emerging role of cold atmospheric plasma in implantology: a review of the literature, Nanomaterials. 10 (2020) 1505, https://doi.org/10.3390/nano10081505.

[18] D. Brány, D. Dvorská, E. Halašová, H. Škovierová, Cold atmospheric plasma: a powerful tool for modern medicine, Int. J. Mol. Sci. 21 (2020) 2932, https://doi.org/10.3390/ijms21082932.

[19] M. Zheng, Y. Yang, X.Q. Liu, M.Y. Liu, X.F. Zhang, X. Wang, et al., Enhanced biological behavior of in vitro human gingival fibroblasts on cold plasma-treated zirconia, PLoS One 10 (2015), e0140278, https://doi.org/10.1371/journal.pone.0140278.

[20] Y. Yang, M. Zheng, Y. Yang, J. Li, Y.-F. Su, H.-P. Li, et al., Inhibition of bacterial growth on zirconia abutment with a helium cold atmospheric plasma jet treatment, Clin. Oral Investig. 24 (2020) 1465–1477, https://doi.org/10.1007/s00784-019-03179-2.

[21] S.J. Lee, D. Yan, X. Zhou, H. Cui, T. Esworthy, S.Y. Hann, et al., Integrating cold atmospheric plasma with 3D printed bioactive nanocomposite scaffold for cartilage regeneration, Mater. Sci. Eng. C Mater. Biol. Appl. 111 (2020) 110844, https://doi.org/10.1016/j.msec.2020.110844.

[22] B. Ezraty, A. Gennaris, F. Barras, J.-F. Collet, Oxidative stress, protein damage and repair in bacteria, Nat Revi Microbiol. 15 (2017) 385–396, https://doi.org/10.1038/nrmicro.2017.26.

[23] H. Van Acker, T. Coenye, The role of reactive oxygen species in antibiotic-mediated killing of bacteria, Trends Microbiol. 25 (2017) 456–466, https://doi.org/10.1016/j.tim.2016.12.008.

[24] L. Han, S. Patil, D. Boehm, V. Milosavljević, P.J. Cullen, P. Bourke, et al., Mechanisms of inactivation by high-voltage atmospheric cold plasma differ for escherichia coli and staphylococcus aureus, Appl. Environ. Microbiol. 82 (2016) 450–458, https://doi.org/10.1128/AEM.02660-15.

[25] G.E. Salvi, D.D. Bosshardt, N.P. Lang, I. Abrahamsson, T. Berglundh, J. Lindhe, et al., Temporal sequence of hard and soft tissue healing around titanium dental implants, Periodontol 2000 (68) (2015) 135–152, https://doi.org/10.1111/prd.12054.

[26] C Park, S-W Park, K-D Yun, M-K Ji, S Kim, Y Yang, et al, Effect of plasma treatment and its post process duration on shear bonding strength and antibacterial effect of dental zirconia, Materials. 11 (2018)2233. doi:https://doi.org/10.3390/ma11112233.

[27] V Vilas Boas Fernandes Júnior, DC Barbosa Dantas, E Bresciani, MF Rocha Lima Huhtala, Evaluation of the bond strength and characteristics of zirconia after different surface treatments, J Prosthet Dent. 120 (2018) 955–959. doi:https://doi.org/10.1016/j.prosdent.2018.01.029.

[28] D. Li, G. Li, J. Li, Z.-Q. Liu, X. Zhang, Y. Zhang, et al., Promotion of wound healing of genetic diabetic mice treated by a cold atmospheric plasma jet, IEEE T Plasma Sci. 47 (2019) 4848–4860, https://doi.org/10.1109/TPS.2019.2928320.

[29] S.-Y. Sun, N-acetylcysteine, reactive oxygen species and beyond, Cancer Bio Ther. 9 (2010) 109–110, https://doi.org/10.4161/cbt.9.2.10583.

[30] J.L. Zimmermann, T. Shimizu, H.U. Schmidt, Y.F. Li, G.E. Morfill, G. Isbary, Test for bacterial resistance build-up against plasma treatment, New J. Phys. 14 (2012), 073037, https://doi.org/10.1088/1367-2630/14/7/073037.

[31] E. Sysolyatina, A. Mukhachev, M. Yurova, M. Grushin, V. Karalnik, A. Petryakov, et al., Role of the charged particles in bacteria inactivation by plasma of a positive and negative corona in ambient air, Plasma Process. Polym. 11 (2014) 315–334, https://doi.org/10.1002/ppap.201300041.

[32] M. Uyen, Surface free energies of oral streptococci and their adhesion to solids, FEMS Microbiol. Lett. 30 (1985) 103–106, https://doi.org/10.1111/j.1574-6968.1985.tb00993.x.

[33] J.A. Imlay, Where in the world do bacteria experience oxidative stress? Environ. Microbiol. 21 (2019) 521–530, https://doi.org/10.1111/1462-2920.14445.

[34] N. Kajarabille, G.O. Latunde-Dada, Programmed cell-death by ferroptosis: antioxidants as mitigators, Int. J. Mol. Sci. 20 (2019) 4968, https://doi.org/10.3390/ijms20194968.

[35] Z. Song, Y. Wu, H. Wang, H. Han, Synergistic antibacterial effects of curcumin modified silver nanoparticles through ROS-mediated pathways, Mater. Sci. Eng. C Mater. Biol. Appl. 99 (2019) 255–263, https://doi.org/10.1016/j.msec.2018.12.053.

[36] J. Li, H. Zhou, J. Wang, D. Wang, R. Shen, X. Zhang, et al., Oxidative stress-mediated selective antimicrobial ability of nano-VO2 against Gram-positive bacteria for environmental and biomedical applications, Nanoscale. 8 (2016) 11907–11923, https://doi.org/10.1039/c6nr02844f.

[37] A. Sculean, R. Gruber, D.D. Bosshardt, Soft tissue wound healing around teeth and dental implants, J. Clin. Periodontol. 41 (Suppl. 15) (2014) S6–S22, https://doi.org/10.1111/jcpe.12206.

[38] F. Rupp, R.A. Gittens, L. Scheideler, A. Marmur, B.D. Boyan, Z. Schwartz, et al., A review on the wettability of dental implant surfaces I: theoretical and experimental aspects, Acta Biomater. 10 (2014) 2894–2906, https://doi.org/10.1016/j.actbio.2014.02.040.

[39] T. Monetta, A. Scala, C. Malmo, F. Bellucci, Antibacterial activity of cold plasma—treated titanium alloy, Plasma Med. 1 (2011) 205–214, https://doi.org/10.1615/PlasmaMed.v1.i3-4.30.

[40] S.-H. Choi, W.-S. Jeong, W.-J. Cha, J.-H. Lee, H.-S. Yu, E.-H. Choi, et al., Time-dependent effects of ultraviolet and nonthermal atmospheric pressure plasma on the biological activity of titanium, Sci. Rep. 6 (2016) 33421, https://doi.org/10.1038/srep33421.

[41] M. Hashmi, S. Ullah, I.S. Kim, Electrospun Momordica charantia incorporated polyvinyl alcohol (PVA) nanofibers for antibacterial applications, Mater Today Commun. 24 (2020) 101161, https://doi.org/10.1016/j.mtcomm.2020.101161.

[42] A. Ullah, S. Ullah, M.Q. Khan, M. Hashmi, P.D. Nam, Y. Kato, et al., Manuka honey incorporated cellulose acetate nanofibrous mats: fabrication and in vitro evaluation as a potential wound dressing, Int. J. Biol. Macromol. 155 (2020) 479–489, https://doi.org/10.1016/j.ijbiomac.2020.03.237.

[43] B. Zhao, H.C. van der Mei, G. Subbiahdoss, J. de Vries, M. Rustema-Abbing, R. Kuijer, et al., Soft tissue integration versus early biofilm formation on different dental implant materials, Dent. Mater. 30 (2014) 716–727, https://doi.org/10.1016/j.dental.2014.04.001.